RSC Advances

This is an *Accepted Manuscript*, which has been through the Royal Society of Chemistry peer review process and has been accepted for publication.

Accepted Manuscripts are published online shortly after acceptance, before technical editing, formatting and proof reading. Using this free service, authors can make their results available to the community, in citable form, before we publish the edited article. This *Accepted Manuscript* will be replaced by the edited, formatted and paginated article as soon as this is available.

You can find more information about *Accepted Manuscripts* in the Information for Authors.

Please note that technical editing may introduce minor changes to the text and/or graphics, which may alter content. The journal's standard Terms & Conditions and the Ethical guidelines still apply. In no event shall the Royal Society of Chemistry be held responsible for any errors or omissions in this *Accepted Manuscript* or any consequences arising from the use of any information it contains.

ROYAL SOCIETY OF CHEMISTRY

www.rsc.org/advances

Use of graphene oxide in achieving high overall thermal properties of polymer for printed electronics

Tianle Zhou[a,b*], Fei Liu[a], Katsuaki Suganuma[b] and Shijo Nagao[b]

[a]School of Materials Science and Engineering, Nanjing University of Science and Technology, Nanjing 210094, China

[b]The Institute of Scientific and Industrial Research, Osaka University, Mihogaoka 8-1, Ibaraki, Osaka 567-0047, Japan

Abstract- Heat removal and "simultaneous" thermal stability are vitally important for the high performance and the long-term reliability of printed electronics. However, such demand is challenging because heat-conductive reinforcements also "simultaneously" encourage the thermal expansion/degradation of polymeric materials. To restrict the motion of polymer chains (the key to achieving increased glass transition temperature (T_g) and thus thermal stability enhancement), chemical modifications are often used to intensify the reinforcement/polymer interfacial interactions but they deteriorate the intrinsic conductivity of reinforcements. Here this deadlock is broken. No chemicals are needed. We reveal an inherent superiority of 'thick' graphene oxide nanoplatelet (GONP) in enhancing both the thermal conductivity and also the T_g and its associated dimensional and structural thermal-stability of epoxy, with a particular emphasis on enabling the thermal conductivity-reinforcing capability of GONP to make a "positive" contribution to the thermal stability enhancement of epoxy. The formed strong GONP/epoxy interfacial interaction was verified by "local" mechanical properties investigated using nanoindentation. Such superiority of 'thick' GONP is based on the specialty of layered-structure and thus can be extended to various GONP-like

* Corresponding author, e-mail: ztltianle999@hotmail.com (Tianle Zhou)

RSC Advances Accepted Manuscript

reinforcements for endowing polymeric materials with high overall thermal properties for printed electronics.

1. Introduction

The surging field of printed electronics offers a promising technology for the fabrication of novel electronic devices, spanning wide applications in lighting, displays, photovoltaics, integrated smart systems, and other electronics and components [1-3]. It imposes high requirement on the heat removal (as better as possible [1]) for preventing organic semiconductor devices (OSDs, slathered for their thin, lightweight and flexible features suitable for printed electronics [1,4]) as well as thermally-sensitive substrates [2] from heating up. Many of OSDs are highly susceptible to heat (for example, thermal vibration/rotation of molecules retards the charge hopping of organic field effect transistors [1, 4]) and thermal cycling is one of their major failure modes, therefore, for the benefit of the high performance and the long-term reliability of plastic electronics, heat-conductive reinforcements are essential [1-3]. In addition, warpage/cracking (caused by thermal expansion stress) and thermal degradation also damage the printed electronic devices. Heat removal and “simultaneous” dimensional and structural thermal -stability are thus vitally important [1]. However, such demand puts those researchers devoted to the material design for printed electronics into a dilemma, because heat-conductive reinforcements also encourage the thermal expansion/degradation of polymeric materials.

Carbon nanomaterials are highly attractive for their exceptional thermal properties. Conventional carbon nanomaterials, such as amorphous carbon and carbon nanotubes (CNTs) [5], have been used to reinforce polymeric materials [6]. Currently, Graphene oxide (GO), definition of which covers from 100nm-thick carbon platelet down to mono

RSC Advances Accepted Manuscript

-layer carbon sheet [7], is particularly intriguing for its two-dimensional (2D) structure (more effective in facilitating the formation of heat-conductive pathways than 1D CNTs) and oxygen-containing groups (facilitating GO dispersion and improving GO/polymer interface). To date, GO, derived from graphite oxide, can be manufactured on the ton scale at low cost [8], making it a promising replacement to CNTs [6]. Lots of methods have been developed to synthesize polymer composites with GO for harnessing its useful properties [6]. For example, GO improved the thermal conductivity [9-18] as well as the dimensional [11, 13, 16] and structural [9, 12, 16, 19-21] thermal-stability of epoxy (the most commonly used adhesive matrix in printed electronics [1]). However, "simultaneously" improving overall thermal properties of polymers for printed electronics with the use of GO still necessitates a deep understanding.

Change in glass transition temperature (T_g) is important because it yields an insight into the variation in polymer dynamics and its associated gain in the thermal stability of polymers. Recently, chemical blending process involving chemical reactions, such as using chemically modified GO or *in-situ* polymerization of monomers in the presence of GO, was reviewed to yield T_g increase (the intensified interfacial interactions exert an enhanced restriction on the motion of polymer chains) [22]. Chemical modifications (such as using 4,4'-diaminodiphenyl sulphone [9], diglycidyl ether of bisphenol-A (DGEBA) [20], or thermotropic liquid crystalline epoxy [21]) upon GO did improve the T_g and the structural thermal-stability of epoxy, but chemical modifications are known to deteriorate the intrinsic conductivity of reinforcements [23]. As far as the *in-situ* thermal cure of epoxy is concerned, GO not only "attends" the cure reaction (-OH groups of GO react with epoxy, establishing interfacial H-bonds) but also "affects" the "thermal" cure process owing to its excellent thermal conductivity (cure reaction

RSC Advances Accepted Manuscript

preferentially occurs around GO chains, the preferred heat-flow pathways) [16], however, hardly any published papers are available to provide an insight into the use of such "thermal conductivity-based effect" of GO in improving T_g and its associated thermal stability of epoxy.

To improve the thermal conductivity of polymers, utilizing GO with large average lateral size (L) has been a consensus reached for continuous heat-conductive pathways with less GO-GO and GO-matrix interfacial thermal resistances. But large-L GO not necessarily gives the optimal reinforcement, the average thickness (λ) of GO is also vital, for example, the thermal conductivity of GO (λ<2nm)/epoxy composites climbed to 6.44 W/mK with 25vol% GO (L= 0.35μm) [10] but only to 0.493 W/mK at a very low maximum loading, 0.5vol%, of GO (L= 10-15μm) [9], so favorable combinations of L and λ necessitate studies. Analysis of the data published calls into a simple classification according to the λ level of GO for the reinforcement of the thermal conductivity of epoxy: (I) ultra-thin (<2 nm) [9-11], (II) 2-10nm [12-16], and (III) 10-100nm [17, 18]. Ultra-thin/-large GO induces the problem of dispersion, GO nanoplatelets (GONPs) with $\lambda_{(II-III)}$ and intermediate L are thus more desirable [24]. With comparable L, GONP (λ_{II}) owns a higher aspect ratio but is flexible (due to its smaller thickness as well as the accompanied more functional groups and structure defects [25]), presenting higher tendency to wrinkle/scroll (2D crystal is thermodynamically unstable, as pointed out by Mermin-Wagner theorem [26]) with both dimensionality and "effective" aspect ratio reduced [27]. By contrast, GONP (λ_{III}) is more rigid (for its higher stiffness with more graphene layers contained [25]) but has a lower intrinsic aspect ratio. So far, for GONPs with comparable intermediate L, hardly any studies are available with more favorable λ level, λ_{II} or λ_{III}, not clear yet.

RSC Advances Accepted Manuscript

To address these problems, here, un-chemically modified GONPs with comparable L but two different λ level i.e. r-GONP (λ_{III}=34nm, L=17μm) and f-GONP (λ_{II}=7nm, L=19μm) are utilized to reinforce epoxy via *in-situ* thermal cure. We reveal an inherent superiority of 'thick' GONP in enhancing the overall thermal properties (both the thermal conductivity and also the T_g and its associated thermal stability) of epoxy, with an emphasis on a thermal conductivity-based "promotion" to the interfacial crosslinking and thus the thermal stability enhancement. This study proposes a chemical-free way for fully exploiting GO in achieving high overall thermal properties of epoxy.

2. Experimental

2.1 Materials

r-GONPs were prepared by the method reported in [23]. f-GONPs were offered by NiSiNa materials Co., Japan. DGEBA with epoxy value of 0.48-0.52mol/100g and the curing agent 2-ethyl-4-methylimidazole (EMI-2,4) were supplied by Shanghai Resin Co., China and Wako Pure Chemical Industries, Ltd., Japan, respectively. The DGEBA/ EMI-2,4 ratio utilized was 100:6, thus etherification reaction during which epoxy molecules crosslink into network dominates the cure reaction [23].

2.2 Preparation of GONP/epoxy composite mixtures and cured composites

GONP/epoxy composite mixtures were fabricated by stirring r-/f-GONP ethanol solution (sonicated for 1.5h in advance), DGEBA and EMI-2,4 together using Mixer ARV310 (Thinky Co., Japan, 1000rpm rotation speed and a simultaneous 2000rpm revolution speed) for 6 times (each time for 5 min). Ice bath was used at intervals to keep the mixture temperature around 283K. GONP loading was 0.5, 1, 2 or 3wt%.

GONP/epoxy composites were fabricated via *in-situ* thermal cure: (a) casting composite mixture in mould, (b) repeatedly degassing in vacuum drying oven at 313K

RSC Advances Accepted Manuscript

until no air bubble appears on the mixture surface, (c) curing (313K×1h, 378K×1.5h, and 458K×1.5h), and (d) cooling, then demoulding.

2.3 Characterization

Morphological studies were done using transmission electron microscopy (TEM, JEM-3000F and FEI Tecnai G2 20) and field emission scanning electron microscopy (FESEM, JSM-6700F). FTIR spectra were measured by Perkin-Elmer Frontier. Crystal structure was tested by wide angle X-ray diffractometry (WXRD, Rigaku RINT RAPID II, 40kV, 30mA). DSC tests on pure epoxy or composite mixtures were done using NETZSCH 204 F1 system (total heat of reaction (ΔQ) was determined by the area under exothermic peak), after cooling, a second run was performed at 10K/min to determine DSC T_g (the midpoint of heat flow step of the second diagram). Thermal conductivity $\kappa = \delta \times C \times \rho$, where thermal diffusivity δ, specific heat C and bulk density ρ were measured by NETZSCH LFA 447 system, 204 F1 system and water displacement, respectively.

Nanoindentation tests were done on a Hysitron TI950 system (load resolution<1nN, displacement resolution<0.04nm, a Berkowich nanoindenter with tip radium<20nm) in a force-control mode with a loading function (a 5-s linear loading and a 5-s unloading segment together with a 5-s holding time of peak load for reducing creep effect). Array of 6×6 tests was performed in 10 random locations (space between arrays>2mm, space between indentations>100μm, great enough to eliminate mutual influences [28]). H and Er were got by analyzing the load-displacement curves with Oliver and Pharr's method [28]. Plasticity index (ψ)= $(A_1-A_2)/A_1$ where A_1 and A_2 are the areas under loading curve and unloading curve, respectively, presenting the ratio of plastic work to total work including plastic work and viscoelastic recovery. In addition, recent study on the rationale of indentation size effect (ISE) in epoxy showed that for sharp Berkovich tip

RSC Advances Accepted Manuscript

(radius<20nm), ISE is negligible as indentation displacement>250nm [29]. To evaluate ISE in this work, indentation tests were done on the epoxy containing the minimum number of nanoplatelets (i.e. 0.5wt% r-GONPs). The loading force was reduced from 5 to 0.5mN on a 1×50 array with the indentation displacement>320nm, such tests were repeated in random 10 locations. As seen in Fig.1, *H* and *E*r are almost stabilized at constants (not significantly decrease with increasing displacement), suggesting that (i) ISE is negligible and (ii) enough r-GONPs were affected and the mechanical behavior could represent an average of microstructure [29], therefore, in this work, peak loads were set to be 5 and 1mN. Furthermore, coefficient of thermal expansion (CTE) tests and thermogravimetric analysis (TGA) were conducted using Hitachi SII TMA/SS7100 (tensile mode, 5mN, 303-443K) and NETZSCH TG-DTA200se/h/24/1, respectively.

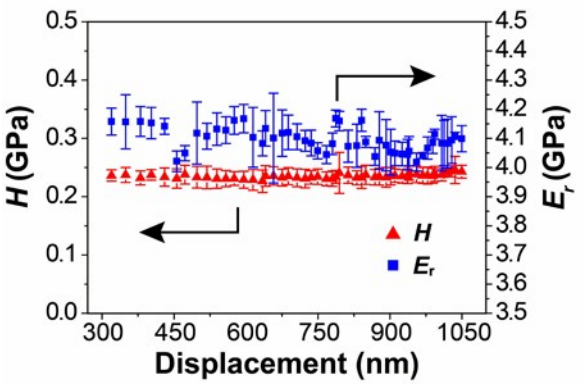

Fig.1 *H* and *E*r of 0.5wt% r-GONP/epoxy composite as a function of indentation displacement.

3. Results and discussion

3.1 Morphology and characterization of r- and f-GONPs

A fluffy opaque r-GONP and a transparent f-GONP are seen in Fig. 2a. Typical TEM image of the core section of r-GONP exhibits ~33.5nm in thickness (see the upper -right inset of Fig. 2a), implying that many r-GONPs used are composed of 33-69

RSC Advances Accepted Manuscript

stacked layers (the average thickness of individually exfoliated GO sheet is ~0.486nm [20]), selected-area electron diffraction (SED) of those stacks shows strong and tense rings (see the bottom-right inset in Fig. 2a), implying a retention of long-range ordering. Meanwhile, the f-GONP presents ~8.2 nm in thickness, associated with 8-17 stacked layers, and SED of the stacks displays only weak and diffuse rings, suggesting a loss of long-range ordering. Statistics survey on 100 platelets based on FESEM images shows that: λ=34nm (5-52nm) and L=17μm (3-30μm) for r-GONPs; λ=7nm (3-13nm) and L=19μm (10-34μm) for f-GONPs.

Furthermore, comparatively rigid r-GONPs while flexible f-GONPs are also observed by FESEM (Fig. 2b). A further study (Fig. 2c) shows that with the decreasing λ, the morphology of GO changes from "flat" platelet (λ=0.5μm) to "valley- and mountain- folded" platelet (λ=32nm), and then to "flexible" platelet (λ=11nm) wrinkled even by 180º fold with edge tending to scroll.

FTIR spectra (Fig. 2d) show that more -OH groups exist on f-GONPs than r-GONPs, evidenced by the more intense band of -OH against -CH band.

RSC Advances Accepted Manuscript

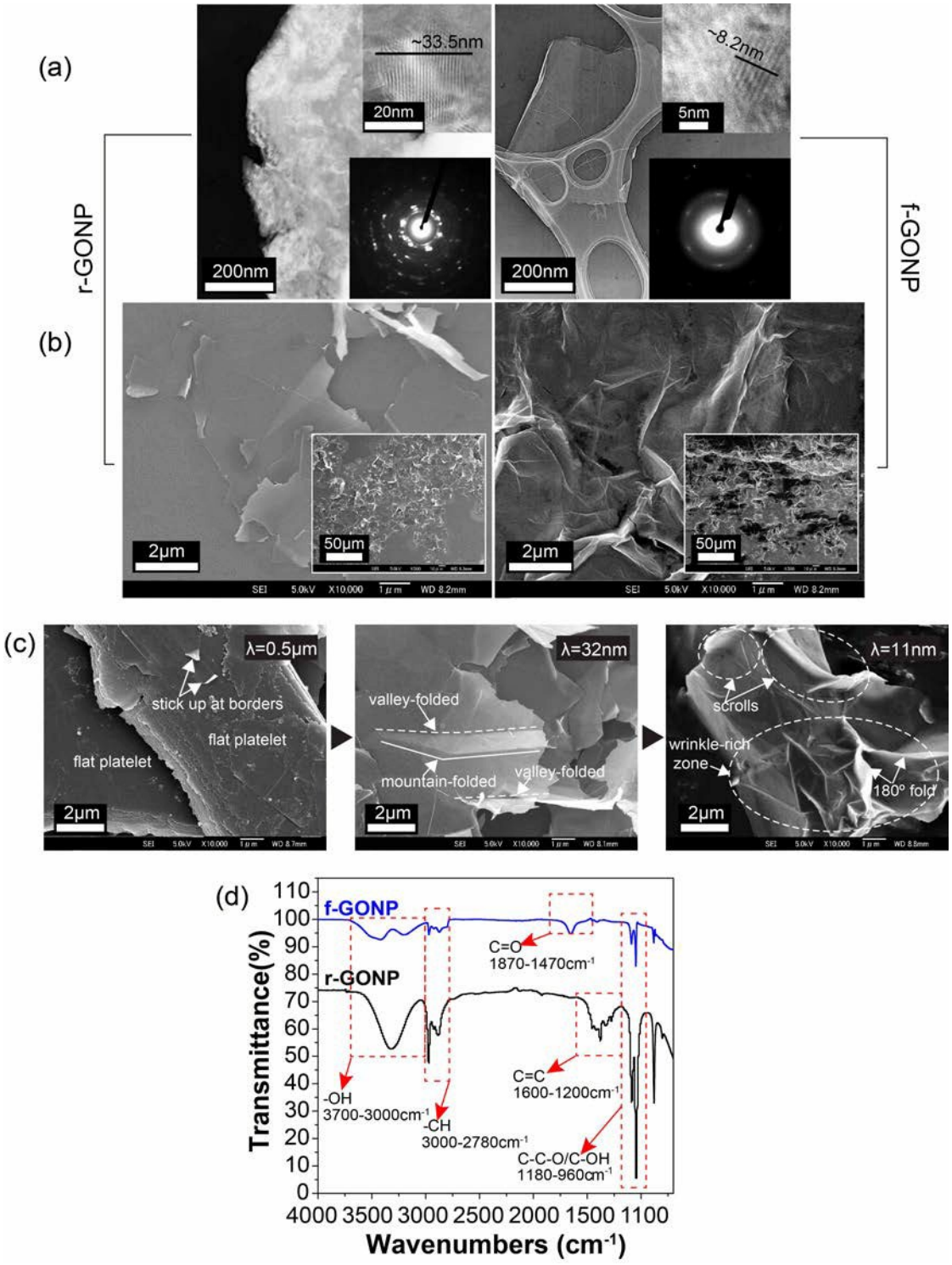

Fig.2 (a) TEM images (insets: cross-section and SED pattern), (b) FESEM images ×10k (insets: ×0.5k), and (d) FTIR spectra of r- and f-GONPs; (c) morphology observation of the waviness as the average thickness λ of GO from 0.5μm down to 11nm.

RSC Advances Accepted Manuscript

3.2 Exfoliation level and dispersion state of r- and f-GONPs in epoxy matrix

WXRD and FESEM are important tools for evaluating the exfoliation level and the dispersion state of GO in matrix, respectively [27].

Fig. 3a presents WXRD patterns of GONPs, epoxy and GONP/epoxy composites. WXRD pattern of r-GONPs exhibits a sharp peak centered at 2θ=26.6° and a small peak at 2θ=43.3°, assigned to the diffraction of (002) and (100) planes of well-ordered graphenes, respectively (the peak at 2θ=26.6° usually shifts to 14.1°-14.9° after oxidization, no shift implies a partial oxidation of r-GONPs (unable to diffraction) [30]). By contrast, WXRD pattern of f-GONPs only shows the small peak and the peak at 2θ=26.6° disappears, indicating a highly exfoliated level of f-GONPs [30]. After r-/f-GONPs were mixed into epoxy, apart from a broad diffraction peak originated from the amorphous epoxy (centered at 2θ=18.5°), r-GONP/epoxy composites only keep a diminished peak at 2θ=26.6°, suggesting a further exfoliation of r-GONPs in matrix; f-GONP/epoxy composites lose the small peak at 2θ=43.3° until 3wt% loading where a tiny peak re-appears (marked by a red circle), suggesting that f-GONPs were fully exfoliated in matrix until f-GONPs restack at 3wt% loading [30].

FESEM images of the fracture surface of 3wt%GONP/epoxy composites (Fig. 3b) shows that the comparatively rigid r-GONPs as well as the tortuous river-like structures by f-GONPs evenly distribute throughout the matrix, no r-/f-GONP agglomerates or holes caused by air bubbles are observed.

Furthermore, TEM images of GONP/epoxy composites (see Fig.3c) confirm that: (i) r-GONPs maintain their layered-structure (though not perfectly parallel-orientated due to partial exfoliation) after they were uniformly dispersed into epoxy matrix, and (ii) f-GONPs were fully exfoliated and evenly dispersed in epoxy matrix until agglomerate

RSC Advances Accepted Manuscript

emerges at 3wt% loading.

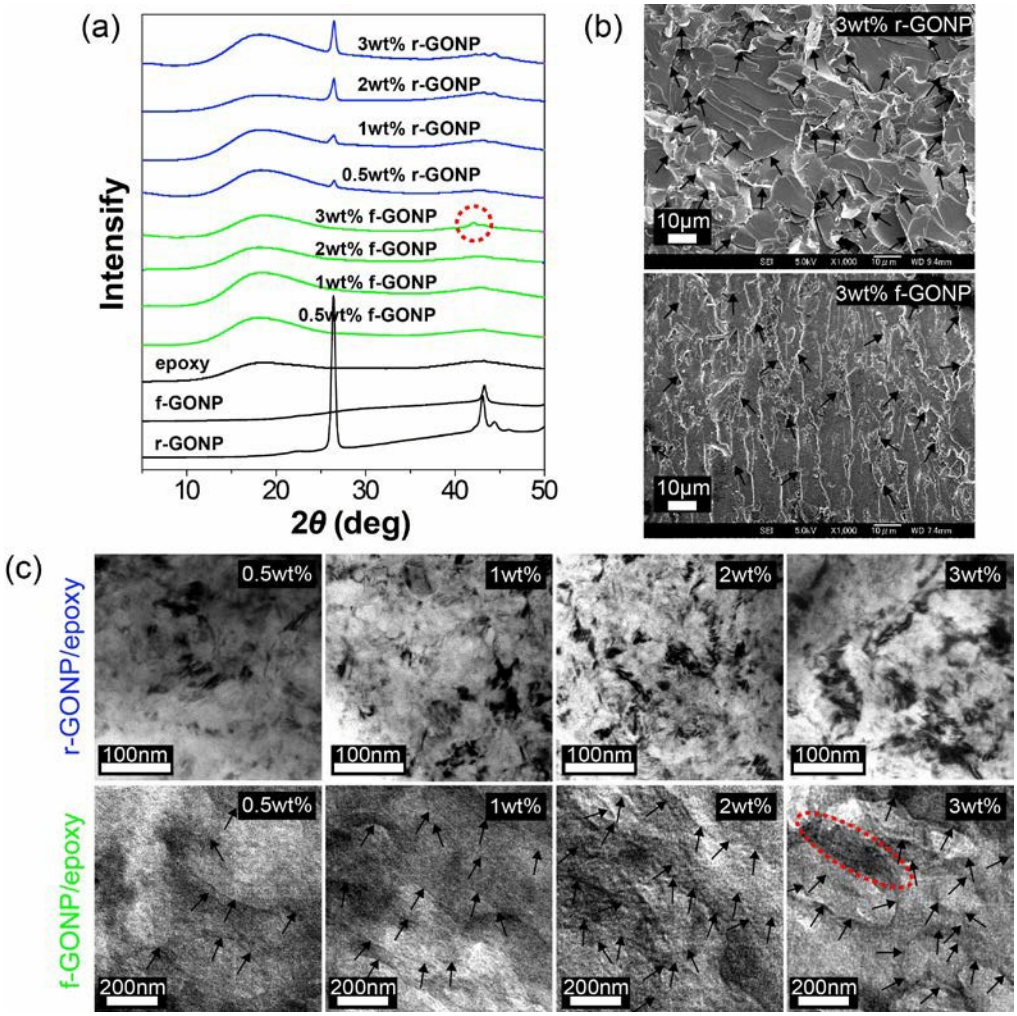

Fig.3 (a) WXRD patterns of GONPs, epoxy and GONP/epoxy composites, circle shows a small peak; (b) FESEM images of the fracture surface of 3wt%GONP/epoxy composites and (c) TEM images of GONP/epoxy composites, arrows show f-GONPs, ellipse shows f-GONP agglomerate.

3.3 The superiority of r-GONP in enhancing the thermal conductivity of epoxy

As seen in Fig. 4a, r-GONP endowed epoxy with higher thermal conductivities than f-GONP. Since the effect of different dispersion state can be ignored (both r- and f-GONPs were well-dispersed in matrix, except 3wt%f-GONP loading), the superiority

RSC Advances Accepted Manuscript

of r-GONP in promoting heat-conduction can be ascribed to the fact: “more” inside-layers acting as the heat-conductive channels, while “less” outside-layers (due to less number of r-GONPs at equivalent wt.% loading) transferring phonons from r-GONPs to epoxy via interfacial H-bonds (in fact, bonded interfaces cause the damping of phonons as matrix is a poor conductor and thus deteriorate the efficiency of conductors [23]).

In addition, some factors further weaken the reinforcing capability of f-GONP: (i) wrinkle/scroll structures of flexible 2D morphology reduce both the dimensionality and the “effective” aspect ratio of f-GONP, as mentioned in Introduction section, (ii) small-wrinkles scatter the phonons with short-wavelength while large-scrolls scatter the long-wavelength phonons [31], and (iii) waviness adds the interfacial thermal resistance (phonon acoustic mismatch rises with the decreasing radius of fillers [10]).

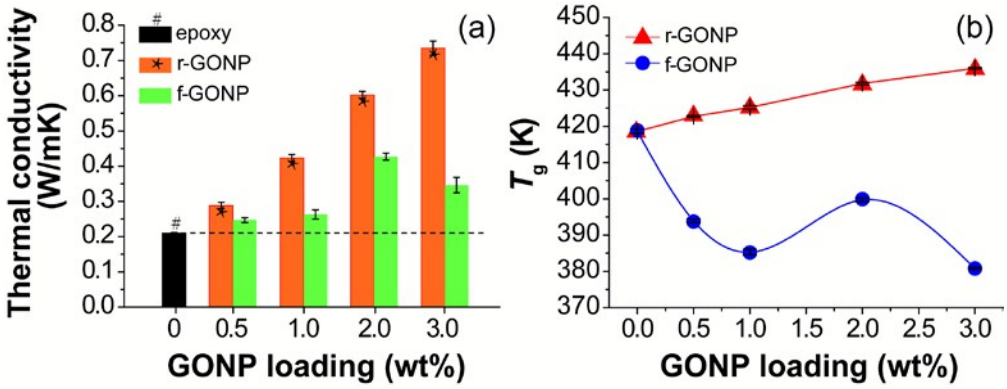

Fig. 4 (a) Thermal conductivities and (b) T_gs of epoxy and GONP/epoxy composites.

It can also be seen in Fig. 4a that the thermal conductivity of f-GONP/epoxy composite rise slowly at low f-GONP contents (flexible morphology makes f-GONPs difficult to form heat-conductive pathways), then it sharply rises to a maximum (2.03 times that of epoxy) at 2wt%f-GONPs (a loading surpassing percolation threshold which falls within 1-2wt% as reported in our previous work [16]), followed by a final decrease at 3wt%f-GONPs (agglomerates emerge and act as phonon scattering sites).

RSC Advances Accepted Manuscript

Meanwhile, the thermal conductivity nearly increases linearly with increasing r-GONP loading, climbing to the maximum (3.5 times that of epoxy) at 3wt% r-GONPs.

More f-GONP loadings e.g. 2.2 and 2.5wt% were also studied in our previous work [16] which proved that further improving the thermal conductivity by increasing the f-GONP loading(>2wt%) is impossible to realize because of the dramatically increased viscosity with big agglomerates and trapped air bubbles impossible to be cleared. In addition, at comparable loading levels, our results with f-GONP are higher than those reported in [14] using GONP (L= ~5μm) with similar λ, such fact can be due to the larger L and thus higher aspect ratio of f-GONP used in this work.

3.4 The superiority of r-GONP in enhancing the T_g of epoxy and an insight offered by DSC and nanoindentation studies

As seen in Fig.4b, r-GONP produced epoxy composites with higher T_gs than f-GONP. 3wt% r-GONPs finally induced a $\Delta T_{g,\,max}$ of 17˚C whereas 3wt% f-GONPs led to a "negative" $\Delta T_{g,\,max}$ of -38˚C. Similar result was reported by the work of Ribeiro et al. [32] where expanded graphite oxide (EGO, tenths to hundreds of GO layers) as well as ultra-thin GO (λ<2nm) functionalized with triethylenetetramine (TETA) enhanced the T_g of epoxy, but no insight into the reinforcing mechanism of EGO was offered. Here, to look insight into the superiority of r-GONP (i.e. 'thick' GONP) in enhancing T_g of epoxy, the *in-situ* thermal cure process of GONP/epoxy systems were monitored with obtained DSC curves shown in Fig.5.

RSC Advances Accepted Manuscript

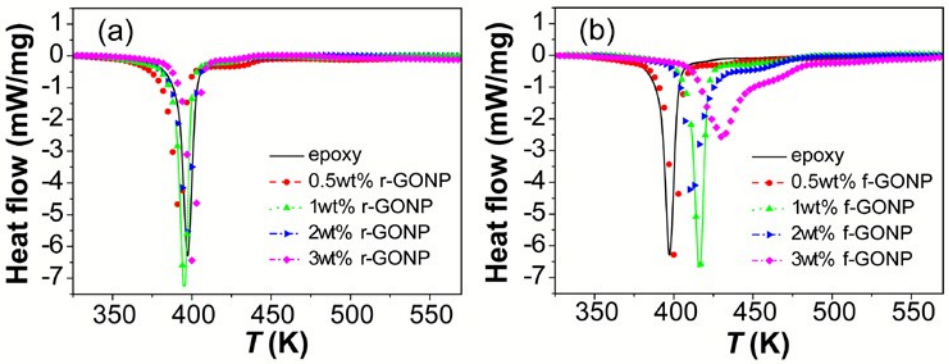

Fig.5 DSC curves at 10K/min heating rate of (a) epoxy and r-GONP/epoxy systems and (b) epoxy and f-GONP/epoxy systems.

3.4.1 DSC study, revealing a "thermal conductivity-based promotion" of r-GONPs to the vitrification transition and thus the T_g increase

The extent of cure reaction (α) *vs*. temperature (T), calculated from DSC curves, is given in Fig. 6a, $\alpha=\Delta Q_T/\Delta Q=S_T/S$ ($0\leq\alpha\leq1$) (total area S of the exothermal peak is in direct proportion to ΔQ). For each formulation all the curves have the same functional form and should be superposable by simply shifting each curve along the T axis relative to a curve at an arbitrary reference heating rate by a shift factor, $\varphi(\upsilon)= T_{ref} -T_\upsilon$, where υ is the heating rate [33]. The superposed curves of α *vs*. T taking the curve of 25K/min heating rate as the master curve are illustrated in Fig. 6b.

RSC Advances Accepted Manuscript

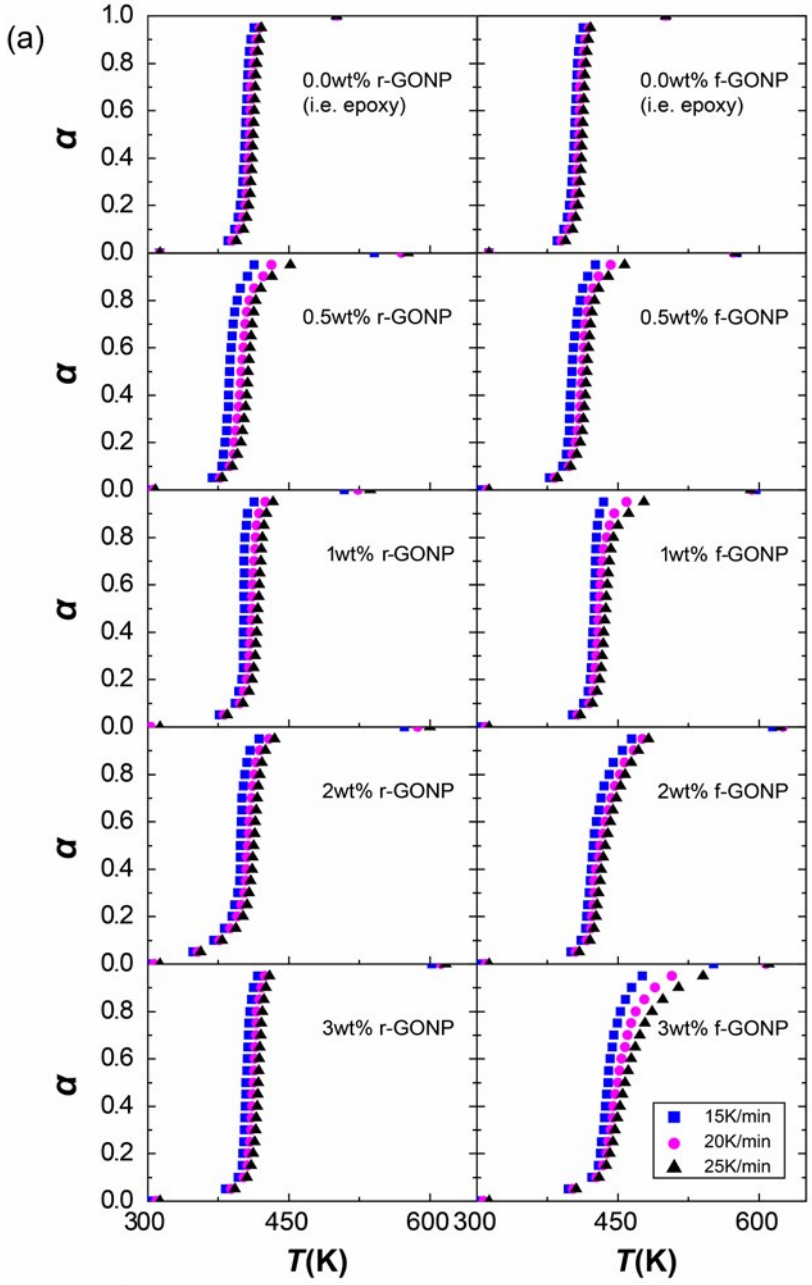

RSC Advances Accepted Manuscript

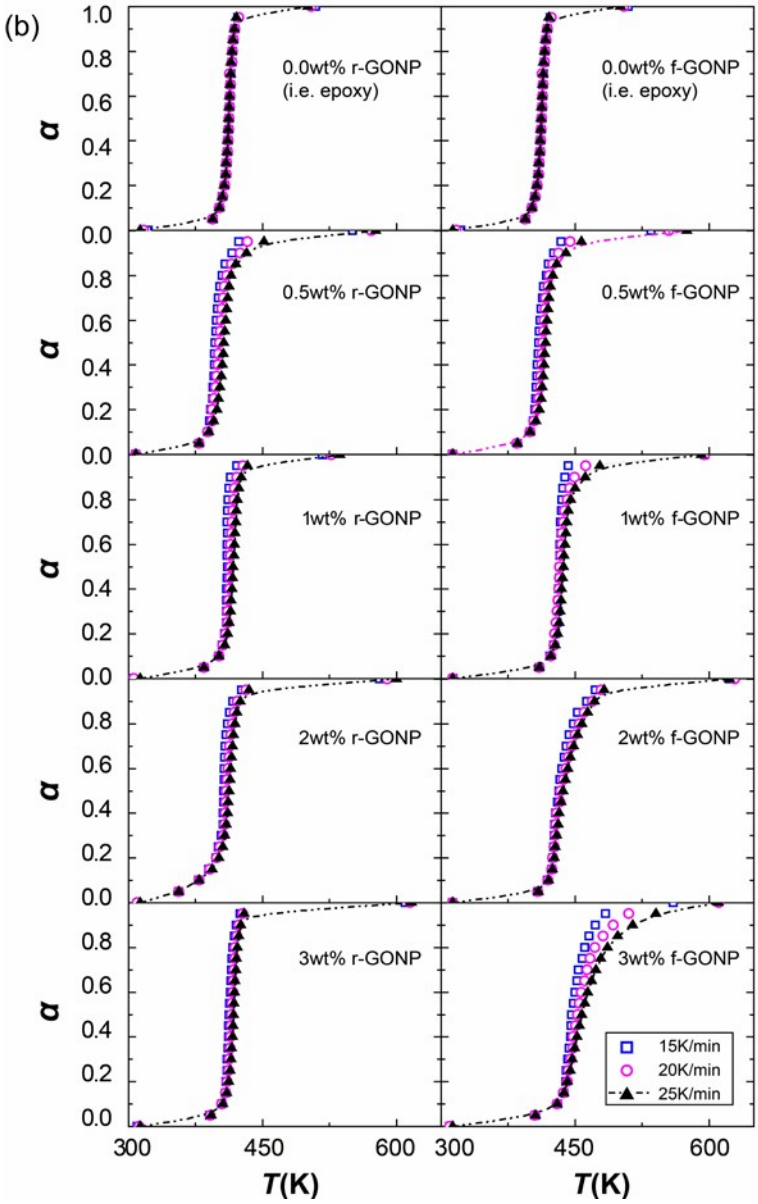

Fig.6 (a) α vs. T and (b) superposed curves of α vs. T of epoxy and GONP/epoxy systems.

The phenomenological reaction rate, $d\alpha/dt$, has a general expression [33]:

$$d\alpha/dt = Ae^{-B/RT}f(\alpha)$$

where A is the frequency factor, B is the activation energy, $f(\alpha)$ is a function of reaction extent α, R is the gas constant and T is the absolute temperature at time t.

let $T = \upsilon t$, then $d\alpha/dT$ can be expressed as:

RSC Advances Accepted Manuscript

$$d\alpha/dT = Ae^{-B/RT}f(\alpha)/\upsilon$$

$$\ln(d\alpha/dT)-\ln[Af(\alpha)] = -B/RT-\ln\upsilon$$

As far as some arbitrary α is concerned, the values of $\ln[Af(\alpha)]$ at different heating rates are equal while the values of $d\alpha/dT_\upsilon$, the tangent slope of the point corresponding to α in the curves at different heating rates, are not always equal to that of the reference curve (i.e. $d\alpha/dT_{ref}$). It has been proved that if the cure reaction is kinetically-controlled, $d\alpha/dT_\upsilon > d\alpha/dT_{ref}$ as taking the curve of maximum heating rate as the master curve, that is to say, the curves of α *vs*. T should branch off from the master curve, and the shift factor $\varphi(\upsilon)=T_{ref}-T_\upsilon$ will increase as α increases[33].

During cure, as T_g increases over curing temperature T_c, system vitrifies (undergoes rubber-to-glass transition), the cure reaction changes from being kinetically-controlled to diffusion-controlled, the values of $d\alpha/dT_\beta$ decrease, i.e. curves of α vs. T do not shift enough from the master curve, although we do not know the exact degree to which the curves should shift from the master curve, a qualitative comparison can be made [33]. As far as the curves in Fig. 6b are concerned, the vitrification degree of r-GONP/epoxy composites follows a sequence 0.5wt%<1wt%<2wt%<3wt%<neat epoxy while that of f-GONP/epoxy composites follows 3wt%<1wt%<0.5wt%<2wt%< neat epoxy, that is to say, at the "later" curing stage, the vitrification transition is promoted with increasing r-GONP loading but is hindered by increasing f-GONP loading (leaving out 2wt% loading), which leads to the higher T_gs by r-GONP.

It is worth noting that (i) the hindrance effect on vitrification transition by f-GONP is baffled at 2wt% loading, (ii) the hindrance by f-GONP on the "initial" curing stage (reflected by the increased exothermic peak temperatures (T_ps) shown in Fig. 7a) is also baffled at 2wt% loading, the critical loading giving a sharp rise in thermal conductivity,

RSC Advances Accepted Manuscript

and (iii) more "promotion" effect on the "initial" curing stage is offered by r-GONP. All these facts highlight a "thermal conductivity-based promotion" of r-GONP to "thermal" cure process (especially the vitrification transition) and thus the final T_g increases.

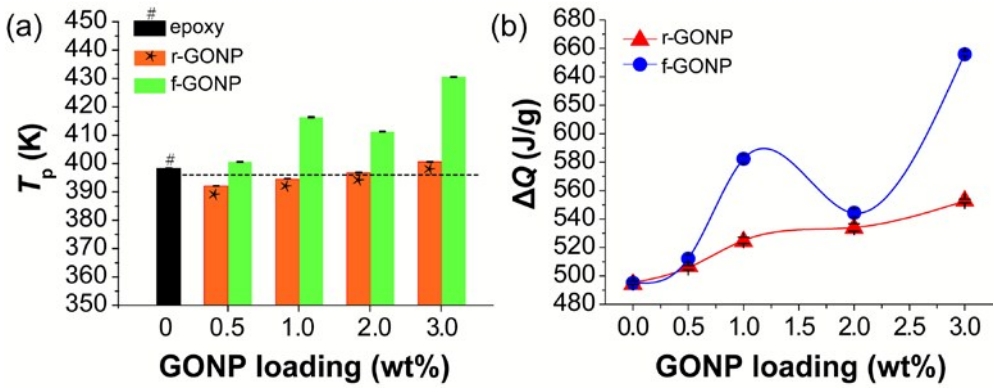

Fig.7 (a) T_ps and (b) ΔQs of DSC curves at 10K/min heating rate of epoxy and GONP/epoxy systems.

The superiority of r-GONP in enhancing the T_g of epoxy can be explained from the perspective of "polymer dynamics" as mentioned in Introduction section. Adding GO has a negative effect on T_g due to a decreased restriction on epoxy motion (epoxy matrix crosslinking is disrupted), and the final T_g can be increased only if strong GO/epoxy interface forms [22]. Compared to f-GONPs, less matrix disruption (due to less number of r-GONPs at equivalent wt.% loading) but more effective interfacial crosslinking "thermally-stimulated" by r-GONPs makes it easier to form enough interfacial H-bonds covering the matrix disruption and enhance local T_g over T_c [22] (supported by the fact that less H-bonds were formed across the r-GONP/epoxy interface as indicated by ΔQ(epoxy)<ΔQ(r-GONP/epoxy systems)<ΔQ(f-GONP/epoxy systems) seen in Fig.7b), then the higher temperature-gradient derived from r-GONPs more efficiently drives the cure reaction into r-GONP-poor zone, resulting in the promoted vitrification transition and higher global T_gs of r-GONP/epoxy composites [16, 22].

RSC Advances Accepted Manuscript

To examine whether stronger r-GONP/epoxy interface forms, nanoindentation, the most sensitive tool in evaluating the reinforcing effect of GO on the “local” mechanical properties of matrix [28] was utilized.

3.4.2 Nanoindentation analysis, verifying a stronger r-GONP/epoxy interface

Typical load-displacement curves and the derived values of H, Er and ψ are presented in Fig. 8. The values of H, Er and ψ of epoxy and 0.5wt% f-GONP/epoxy composite are comparable with those reported in [34] where GONPs has λ of 6-8nm, similar to f-GONPs used in this work.

RSC Advances Accepted Manuscript

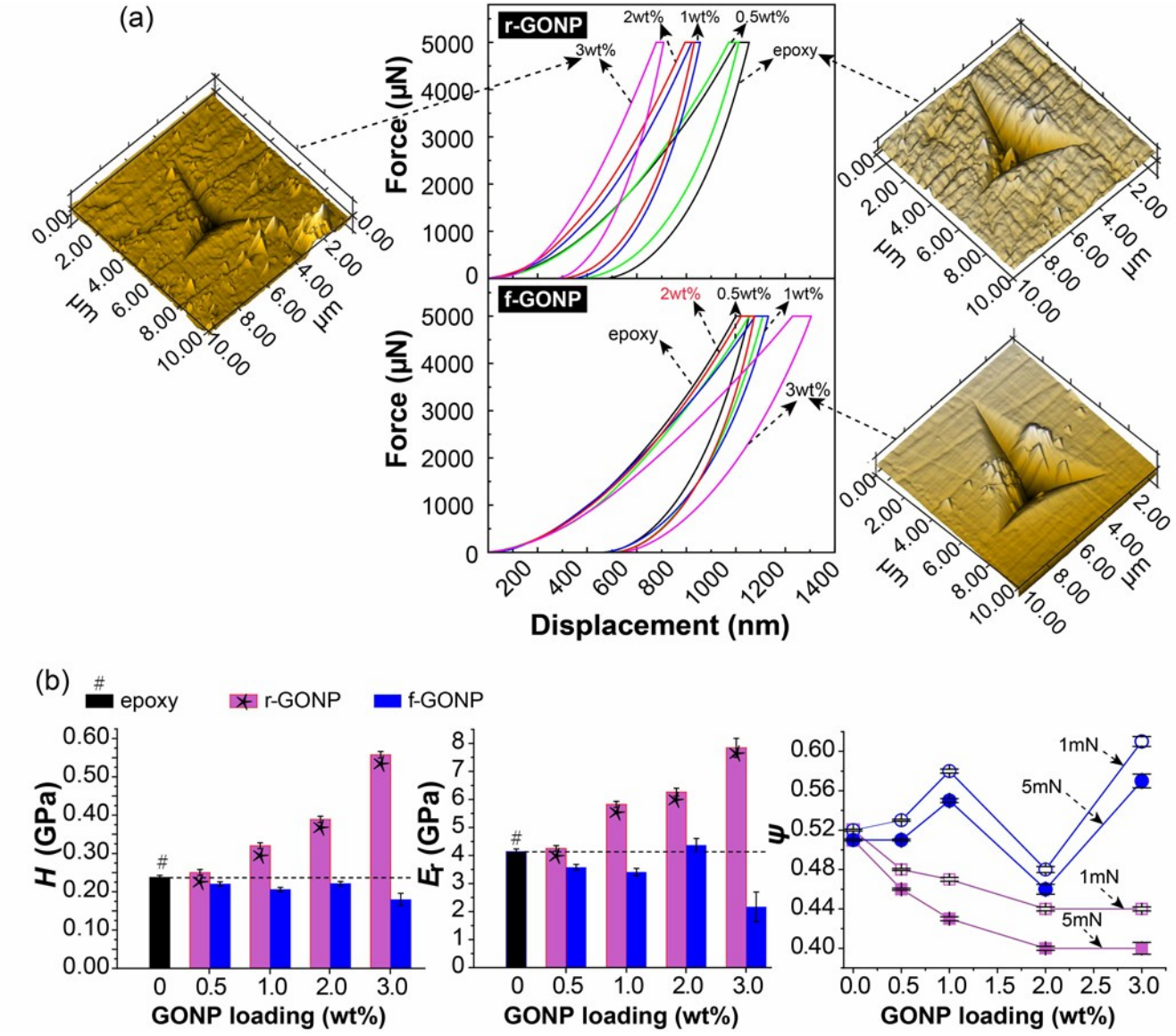

Fig.8 (a) Typical load-displacement curves of epoxy and GONP/epoxy composites (insets: atomic force microscopy (AFM) images of the indentation locations), (b) H, E_r and ψ as a function of GONP loading.

Theoretical [35] and experimental [36] works have shown that: (i) H=0.95TPa and Er= 0.89TPa for mono-layer graphene, (ii) H and Er drop as the graphene layer number increases, and (iii) Er approaches the constant of bulk graphite (~27 GPa) as λ>six layers. Accordingly, H(r-GONP)<H(f-GONP) and Er(r-GONP)=Er(f-GONP). For the

RSC Advances Accepted Manuscript

materials with viscoelastic-plastic behavior, $0<\psi<1$ and ψ(r-GONP)= ψ(f-GONP) (due to an absence of cellular structure of exfoliated r-GONPs in epoxy) [37]. Based on these facts, interesting results are noticed in Fig. 8:

(1) *H*(r-GONP/epoxy composites)>*H*(epoxy)>*H*(f-GONP/epoxy composites), with indentation curves in Fig. 8a shifting to the left as increasing the r-GONP loading but to the right when adding f-GONPs.

It is known that (i) poor GONP/epoxy interface weakens the load transfer, and (ii) partial exfoliation or poor dispersion of GONPs enables graphene to slip between layers or platelets, respectively (due to the weak van der Waals bonding between layers or platelets), causing a softening effect by slip mechanism [27, 36]. Since full exfoliation as well as good dispersion of f-GONPs in epoxy matrix (except 3wt% loading) has been proved above, *H*(f-GONP/epoxy composites)<*H*(epoxy) can only be ascribed to a poor f-GONP/epoxy interface. By contrast, r-GONPs were well dispersed but partially exfoliated in matrix which brings a negative effect on *H*, however, the final result of *H*(r-GONP/epoxy composites)>*H*(epoxy) can only be attributed to a good r-GONP/ epoxy interface which transfers load effectively.

Ribeiro et al. [32] reported that adding graphene materials into epoxy hardly affects *H*, in fact, analysis on their data comes to a similar trend: *H*(3wt%EGO/epoxy composite)>*H*(epoxy)>*H*(TETA-3wt%f-GONP/epoxy composite). Compared with our results, their less increase in *H* can be ascribed to the ultra-thickness of EGO, and their less decrease in *H* by f-GONP can be due to the enhanced interface by TETA treatment.

(2) *E*r(r-GONP/epoxy composites)>*E*r(epoxy)>*E*r(f-GONP/epoxy composites), regardless of 2wt% loading of f-GONPs.

This result shows that r-GONP/epoxy composites also exhibit the best elastic

RSC Advances Accepted Manuscript

recovery after deformation, thus confirming a stronger r-GONP/epoxy interface which effectively restricts the motion of epoxy chains.

(3) ψ(r-GONP/epoxy composites)<ψ(epoxy)<ψ(f-GONP/epoxy composites), regardless of 2wt% loading of f-GONPs.

It can be seen in Fig. 8b that both the r-GONP/epoxy composites and the f-GONP/ epoxy composites exhibit a reduction in ψ as increasing the load force from 1 to 5mN. Such result is associated with "the higher force, the deeper indentation". Bulk macromolecules are harder to respond to the external load and are also more effectively pulled back to their original configuration upon unloading due to a stronger interaction in bulk than near surface, consequently, less plastic deformation remains with ψ reduced [27]. For a similar reason, ψ(r-GONP/epoxy composites)<ψ(f-GONP/epoxy composites) as well as the smallest residual hole in AFM image (see Fig. 8a) reconfirms a stronger r-GONP/ epoxy interfacial interaction.

Besides, the "abnormal" increase in H and Er, as well as the "abnormal" decrease in ψ, at 2wt%f-GONPs loading reconfirms the "thermal conductivity-based promotion" of GONPs to interfacial crosslinking and thus the resulting strengthened interface.

3.5 Verifying the superiority of r-GONP in enhancing the thermal stability of epoxy

T_g-associated gains in dimensional and structural thermal-stability of epoxy upon the incorporation of r-/f-GONPs are compared by testing CTE and TGA, respectively, with the results presented in Fig.9. It is common to consider the half-weight-loss temperature (T_{half}) as the indicator for the beginning of the structural decomposition; therefore, T_{half}s obtained from TGA curves are also illustrated in Fig.9.

RSC Advances Accepted Manuscript

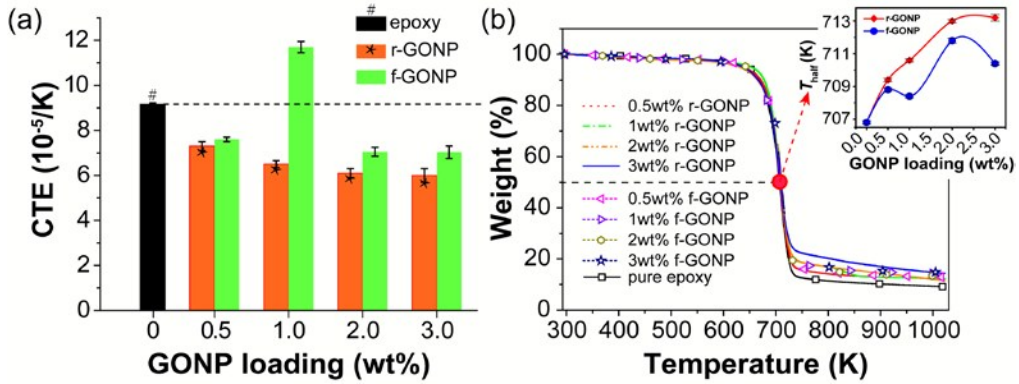

Fig. 9 (a) CTE values and (b) TGA curves (inset: plot of T_{half}s determined from TGA curves) of epoxy and GONP/epoxy composites.

As shown in Fig. 9a, r-GONP endowed epoxy with lower CTE than f-GONP, verifying the superiority of r-GONP in enhancing the dimensional thermal stability of epoxy. CTE of GONP/epoxy composites originates in three parts: epoxy, GONPs and GONP/epoxy interface. It is well-known that CTE (monolayer graphene)<0, and CTE (graphite)>0 (due to the weak van der Waals bonding between graphene layers) but is less than CTE(epoxy) [11]. Accordingly, CTE(f-GONP)<CTE(r-GONP)<CTE(epoxy). It is reasonable to see that CTE of epoxy composites decreases with increasing r-/f-GONP loading (unless losing control over epoxy motion e.g. at 1wt% f-GONP loading). More importantly, CTE(r-GONP)>CTE(f-GONP) but CTE(r-GONP/epoxy composites) <CTE (f-GONP/epoxy composites) also verifies the stronger r-GONP/epoxy interface.

The superiority of r-GONP in enhancing the structural thermal stability is verified as well, based on the fact that higher T_{half}s were achieved by r-GONP (see the inset in Fig. 9b). The incorporated r-/f-GONPs offer barrier to the thermal degradation of epoxy, reflected by the increased T_{half}s ("tortuous" path effect of GONPs limits the entry of oxygen and delays the escape of volatile degradation products [21, 33]). Comparatively, r-GONP offers more thermal-conductive promotion and less tortuous-path hindrance to

RSC Advances Accepted Manuscript

the thermal degradation, but finally it produces higher T_{half}s, this result can only be ascribed to a stronger r-GONP/epoxy interface.

4. Conclusions

Our findings in this study reveal a superiority of 'thick' GONP in endowing epoxy with high overall thermal properties (both the thermal conductivity and also the T_g and its associated dimensional and structural thermal-stability). Taking the advantage of the specialty of thick layered-structure, i.e. less matrix disruption (due to less number of 'thick' GONPs at equivalent wt.% loading) but more effective interfacial crosslinking (thermally stimulated by 'thick' GONP with its higher heat-conductive capability), we first open up a avenue to enable the thermal conductivity-reinforcing capability of GONP to make a "positive" contribution to the thermal stability enhancement of epoxy. Chemicals usually used to strengthen the interfacial interactions for enhanced T_g and thermal stability is unneeded, thus the harm to the intrinsic conductivity of GONP by chemical modifications was successfully avoided. Therefore, this chemical-free avenue by using 'thick' GONP is the way fully exploiting GO in achieving high overall thermal properties of epoxy, and can be applied to various GO-like reinforcements for achieving high overall thermal properties of polymeric materials for printed electronics.

Acknowledgements

The authors are grateful for the financial support of National Natural Science Foundation of China (No.51203074), Fundamental Research Funds for the Central Universities (No. NUST 2011YBXM163), Jiangsu Overseas Research & Training Program for University Prominent Young & Middle-aged Teachers and Presidents, and 'first-grade Zijin's Star' of Nanjing University of Science and Technology (AB41339).

RSC Advances Accepted Manuscript

References

[1] K. Suganuma, *Introduction to printed electronics*, Springer Science & Business Media, New York, USA, 2014.

[2] E. B. Secor, B. Y. Ahn, T. Z. Gao, J. A. Lewis and M.C. Hersam, *Adv. Mater.*, 2015, **27**, 6683-8.

[3] A. Kamyshny and S. Magdassi, *Small*, 2014, **10**, 3515-35.

[4] T. Okamoto, C. Mitsui, M. Yamagishi, K. Nakahara, J. Soeda, Y. Hirose, K. Miwa, H. Sato, A. Yamano, T. Matsushita, T. Uemura and J .Takeya, *Adv. Mater.*, 2013, **25**, 6392-7.

[5] A. Saha, C.Jiang and A. A. Martí, *Carbon*, 2014, **79**, 1-18.

[6] X.Huang, X.Qi, F. Boey and H. Zhang, *Chem. Soc. Rev.*, 2012, **41**, 666-86.

[7] X. Zhuang, Y. Mai, D. Wu, F. Zhang and X. Feng, *Adv. Mater.*, 2015, **27**, 403-27.

[8] M. F. El-Kady, V. Strong, S. Dubin and R. B. Kaner, *Science*, 2012, **335**, 1326-30.

[9] Y. Hu, J. Shen, N. Li, H. Ma, M. Shi, B. Yan, W. Huang, W. Wang and M. Ye, *Compos. Sci. Technol.*, 2010, **70**, 2176-82.

[10] A. Yu, P. Ramesh, M. E. Itkis, E. Bekyarova and R. C. Haddon, *J. Phys. Chem. C.*, 2007, **111**, 7565-9.

[11] S. Wang, M. Tambraparni, J. Qiu, J. Tipton and D. Dean, *Macromolecules*, 2009, **42**, 5251-5.

[12] M. A. Raza, A. V. K. Westwood and C. Stirling, *Mater. Chem. Phys.*, 2012, **132**, 63-73.

[13] B. Ahmadi-Moghadam and F.Taheri, *J. Mater. Sci.*, 2014, **49**, 6180-90.

[14] F. Wang, L. T. Drzal, Y. Qin and Z. Huang, *J. Mater. Sci.*, 2015, **50**, 1082-93.

RSC Advances Accepted Manuscript

[15] J. Kim, B.-S. Yim, J.-M. Kim and J. Kim, *Microelectron. Reliab.*, 2012, **52**, 595-602.

[16] T. Zhou, H. Koga, M. Nogi, T. Sugahara, S. Nagao, T. T. Nge, K. Suganuma, H.-W. Cui, F. Liu and Y. Nishina, *eXPRESS. Polym. Lett.*, 2015, **9**, 608-23.

[17] C. Min, D. Yu, J. Cao, G. Wang and L. Feng, *Carbon*, 2013, **55**, 116-125.

[18] K. Chu, W.-S. Li and H. Dong, *Appl. Phys. A-Mater.*, 2013, **111**, 221-5.

[19] H. Hu, L. Chen and G. Chen, *Mater. Manuf. Process.*, 2011, **26**, 618-22.

[20] Y.-J. Wan, L.-C. Tang, L.-X.Gong, D.Yan, Y.-B. Li, L.-B. Wu, J.-X. Jiang and G.-Q. Lai, *Carbon*, 2014, **69**, 467-480 .

[21] B. Qi, S. R. Lu, X. E. Xiao, L. L. Pan, F. Z. Tan and J. H. Yu, *eXPRESS. Polym. Lett.*, 2014, **8**,467-79.

[22] K.-H. Liao, S. Aoyama, A. A. Abdala and C. Macosko, *Macromolecules*, 2014, **47**, 8311-8319.

[23] T. Zhou, X. Wang, P. Cheng, T. Wang, D. Xiong and X. Wang, *eXPRESS. Polym. Lett.*, 2013, **7**,585-94.

[24] S.G. Prolongo, R. Moriche, A. Jiménez-Suárez, M. Sánchez and A. Ureña, *Eur. Polym. J.*, 2014, **61**, 206-14.

[25] J. Shang, Y. Chen, Y. Zhou, L. Liu, G. Wang, X. Li, J. Kuang, Q. Liu, Z. Dai, H. Miao, L. Zhi and Z. Zhang, *Polymer*, 2015, **68**, 131-9.

[26] M. Annamalai, S. Mathew, M. Jamali, D. Zhan and M. Palaniapan, *J. Phys. D.: Appl. Phys.*, 2013, **46**, 145302.

[27] L-C. Tang, Y-J. Wan, D. Yan, Y-B. Pei, L. Zhao, Y-B. Li, L-B. Wu, J-X. Jiang and G-Q. Lai, *Carbon*, 2013, **60**, 16-27.

[28] A. M. Díez-Pascual, M. A. Gomez-Fatou, F. Ania and A. Flores, *Prog. Mater. Sci.*,

RSC Advances Accepted Manuscript

2015, **67**, 1-94.

[29] F. Alisafaei, C.-S. Han and N. Lakhera, *Polym. Test.*, 2014, **40**, 70-8.

[30] M. Mauro, M. R. Acocella, C. E. Corcione, A. Maffezzoli and G. Guerra, *Polymer*, 2014, **55**, 5612-5.

[31] K. Zhang, Y. Zhang and S. Wang, *Carbon*, 2013, **65**, 105-11.

[32] H. Ribeiro, W. M. Silva, M.-T. F. Rodrigues, J. C. Neves, R. Paniago, C. Fantini, H. D. R. Calado, L. M. Seara and G. G. Silva, *J. Mater. Sci.*, 2013, **48**, 7883-92.

[33] T. Zhou, X. Wang, X. Liu and D. Xiong, *Carbon*, 2009, **47**, 1112-8.

[34] M. M. Shokrieh, M. R. Hosseinkhani, M. R. Naimi-Jamal and H.Tourani, *Polym. Test.*, 2013, **32**, 45-51.

[35] B. Mortazavi, Y. Rémond, S. Ahzi and V. Toniazzo, *Comp. Mater. Sci.*, 2012, **53**, 298-302.

[36] Y. Zhang and C. Pan, *Diam. Relat. Mater.*, 2012, **24**, 1-5.

[37] P.-H. Chen and D. D. L.Chung, *Carbon*, 2015, **81**, 505-13.

RSC Advances Accepted Manuscript

Use of graphene oxide in achieving high overall thermal properties of polymer for printed electronics

GRAPHICAL ABSTRACT

Description

Superiority of 'thick' graphene oxide in simutaneously enhancing both the thermal condcutivity and the dimensional and structural thermal-stability of epoxy

Graphical

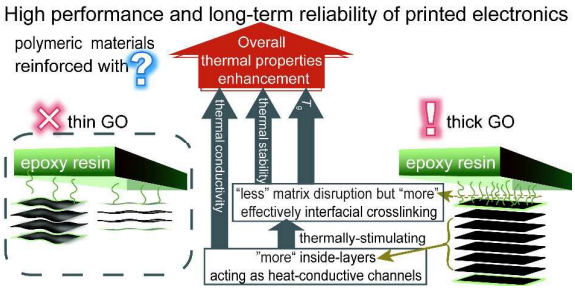

RSC Advances Accepted Manuscript